Research Article | Vol. 28, No. 24 / 23 November 2020 / Optics Express 37058
Optics EXPRESS

Direct detection based φOTDR using the Kramers-Kronig receiver

XIN LU* AND KATERINA KREBBER

Bundesanstalt für Materialforschung und–prüfung (BAM), 12205, Berlin, Germany
*xin.lu@bam.de

Abstract: A Kramers-Kronig (KK) receiver is applied to a phase-sensitive optical time domain reflectometry based on direct detection. An imbalanced Mach-Zehnder interferometer with a 2×2 coupler is used in sensing system to encode the phase information into optical intensity. The directly obtained signal is treated as the in-phase component, and the KK receiver provides the quadrature component by Hilbert transform of the obtained signal, so that the optical phase can be retrieved by IQ demodulation. The working principle is well explained, and the obtained phase variance is theoretically analyzed. The experiment demonstrates the functionality of the sensor and validates the theoretical analysis.

1. Introduction

Phase-sensitive optical time domain reflectometry (φOTDR) has proven to be an effective distributed vibration sensing technique. It exploits a standard optical fiber as the sensing medium and collects the Rayleigh backscattered light of the optical pulses to retrieve the vibration information. The simple configuration and the high performance make the sensing system an excellent candidate for spatially resolved vibration measurement. The φOTDR system has been widely used in oil and gas industry, structural health monitoring, etc. [1].

A vibration will change the local properties (refractive index and inhomogeneity size) of the optical fiber, thus the position and the frequency can be easily determined based on the intensity of the backscattered light, which can be easily detected [2]. However, the applied strain, an interesting parameter in many areas, is difficult to retrieve. Most of the current φOTDR systems use the optical phase to calibrate strain because the vibration causes an extra phase delay of the backscattered light [3–6]. Coherent detection is able to measure both the amplitude and the phase of an optical wave, so it has been applied to φOTDR sensing to quantify strain. In a coherent-detection-based φOTDR system, the beat between the backscattered light and a local oscillator is acquired and the optical phase is usually extracted by IQ demodulation. The in-phase (I) and quadrature (Q) components for the demodulation can be acquired through a 90° hybrid in optical domain [3], or by pure data processing in digital domain [7,8]. Recently, the Kramers-Kronig (KK) receiver has been proposed for coherent detection [9]. It relies on the Kramers-Kronig relation, and acquires the I and Q components from the detected signal in the digital domain [9,10]. The KK receiver has the advantage of high spectral efficiency and low hardware cost, it has therefore been widely used in optical communication and in distributed fiber sensing as well [11]. For coherent detection, the coherence length of the light source must be longer than the sensing distance. Therefore, the light source must possess very narrow linewidth (down to kHz) to achieve a long sensing distance.

The direct-detection-based φOTDR systems can also retrieve the phase information with the help of different interferometers to convert the phase information into intensity. The most used interferometric configurations are the imbalanced Mach-Zehnder interferometer (IMZI) and Michelson interferometer [5,6]. The one path of the interferometer should be longer than the other so that the output is dependent on the phase difference between two fiber positions. The direct detection has a comparatively loose requirement on the linewidth of the light source,

#405723 https://doi.org/10.1364/OE.405723
Journal © 2020 Received 20 Aug 2020; revised 19 Oct 2020; accepted 19 Oct 2020; published 20 Nov 2020

Optics EXPRESS

the corresponding coherence length just needs to be longer than the path length difference, which is equivalent to a MHz linewidth. Differentiation and cross-multiplication (DCM) and IQ demodulation have been used to retrieve the phase difference from the obtained signal [5,12]. Currently, most of the interferometers use a 3×3 coupler as the output, and 3 or at least 2 identical photodetectors are necessary to acquire the optical signal [5,6]. Consequently, the sensor possesses a complex configuration and a small difference between the detectors will have a large influence on the sensing performance. Recently, a φOTDR based on an IMZI with a 2×2 coupler has been proposed and the output of the interferometer is obtained by a balanced photodetector [13]. Such a simple system minimizes the impact of the photodetector difference. However, the phase information is demodulated by the DCM, which is supposed to offer larger phase errors than the IQ demodulation [12].

In this paper, the KK receiver is applied to a φOTDR system based on direct detection for the first time to the best of our knowledge. The phase extraction scheme of the system relies on an IMZI with a 2×2 coupler and IQ demodulation is used to retrieve the phase information based on the I and Q components obtained by the KK receiver. The working principle and the phase error of the proposed system are theoretically analyzed and experimentally validated. Finally, theoretical analysis has been used to show that the IMZI with a 2×2 coupler has a similar performance with that of a 3×3 coupler. The simple configuration and low-cost make the proposed φOTDR system an attractive solution to borehole monitoring, intrusion detection and so on.

2. Theoretical analysis

2.1. Working principle

The φOTDR system relies on the Rayleigh backscattering in an optical fiber. All fibers are not perfectly uniform and consist of enormous inhomogeneities, which exhibit different sizes and densities. Consequently, the refractive index varies randomly along the fiber. In a φOTDR system, optical pulses from a coherent light source are launched into the fiber, and they get continuously deflected at the inhomogeneity during the propagation. A small portion of the light is backscattered and acquired by the sensing system. Actually, the light backscattered within the half pulse length will arrive together at the photodetector, so the system obtains the summation of them, and this process can be seen as optical interference. The result of the interference is certainly dependent on the local refractive index, which has a stochastic distribution, hence the obtained signal exhibits a random value along the fiber. Previous investigations have demonstrated that the amplitude and the intensity of the backscattered light obey Rayleigh and exponential distribution, respectively, and the optical phase is uniformly distributed between –π and π [1,14].

Environmental variations (temperature and strain) will cause the local change of the fiber properties, i.e. inhomogeneity size and density, altering the interference process. Therefore, the amplitude $A(z)$ and phase $\varphi(t, z)$ of the backscattered light $E(t, z)$ is changed, t denotes the measurement time and z represents the position. Note that $A(z)$ represents the amplitude that is dependent only on the incident wavelength, optical power and the local intrinsic refractive index. A recent analysis shows that this amplitude remains the same even under external perturbation within a short time period [15]. Thus, the amplitude $A(z)$ is considered as a time independent variable in this paper, and the obtained signal change is only caused by the environmentally induced phase delay. The strain induced phase delay can be expressed as [16]

$$\varphi_\varepsilon = 2\pi nl/\lambda \cdot \{1 - 1/2 \cdot n^2[(1-\mu)p_{12} - \mu p_{11}]\}\varepsilon, \tag{1}$$

where n is the refractive index of the fiber, l is the length of stretched section, λ is the optical wavelength, ε is the applied strain and μ=0.17 is the Poisson's ratio and the strain-optic coefficients p_{11} and p_{12} are taken as 0.121 and 0.27, respectively. Thus, a phase delay of 9.2 rad is induced by a strain change of 1 με over a fiber section of 1 m when λ=1550 nm.

Optics EXPRESS

The vibration location and frequency can be determined from the amplitude variation, whereas the strain information needs to be calibrated by the phase difference between two positions [17]. In a direct detection based φOTDR system, the phases from two locations are compared by an interferometer so that the phase difference can be extracted directly.

The scheme of an IMZI with a 2×2 coupler is shown in Fig. 1. The Rayleigh backscattered light *E(t, z)* is at first divided evenly by a 50:50 splitter and enters the two arms of the interferometer. The light in the upper arm propagates Δl longer than in the lower arm, thus the optical fields at the entrance of the 2×2 coupler are respectively expressed as

$$\begin{cases} E_A(t,z) = \frac{1}{\sqrt{2}} E(t, z-\Delta l) e^{-j2\pi\Delta l/\lambda} \\ E_B(t,z) = \frac{1}{\sqrt{2}} E(t,z) e^{-j\pi/2} \end{cases}, \tag{2}$$

the factor $1/\sqrt{2}$ and the $\pi/2$ phase shift are caused by the splitter. The length difference Δl between the two arms enables the optical phase comparison at position $z-\Delta l$ and z, and it defines the gauge length. The light E_A and E_B are mixed in the 2×2 coupler and the outputs are written as

$$\begin{cases} E_1(t,z) = \frac{1}{\sqrt{2}} [E_A(t,z) + E_B(t,z) e^{-j\pi/2}] \\ E_2(t,z) = \frac{1}{\sqrt{2}} [E_A(t,z) e^{-j\pi/2} + E_B(t,z)] \end{cases}. \tag{3}$$

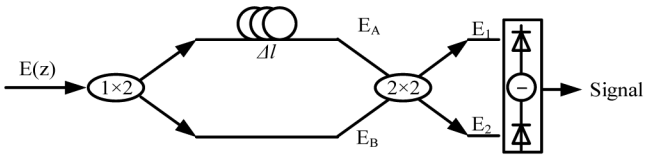

Fig. 1. Optical phase retrieval configuration based on an imbalanced Mach-Zehnder interferometer with a 2×2 coupler. The output of the coupler is connected to a balanced photodetector.

The coupler is connected directly to the two photodiodes of the balanced photodetector. The light beams E_1 and E_2 are converted into electrical signals and their difference is the output of the detector. Note that the whole process is similar to as a special type of homodyne detection, E_1 or E_2 acts as a local oscillator and the other can be seen as the signal. Thus, the beat between E_1 and E_2 is at baseband, unlike the heterodyne detection. And the homodyne detection has a higher spectrum efficiency [11]. The output of the balanced detection can be expressed as

$$\begin{aligned} P_{out}(t,z) &= E_1(t,z)E_1^*(t,z) - E_2(t,z)E_2^*(t,z) \\ &= -|A(z)A(z-\Delta l)| \cos[\Delta\varphi(t,z) - 2\pi\Delta l/\lambda] \end{aligned}, \tag{4}$$

where * denotes the complex conjugation, and $\Delta\varphi(t, z)$ represents the phase difference between two positions as $\Delta\varphi(z)=\varphi(z)-\varphi(z-\Delta l)$. Equation (4) shows that the obtained signal is essentially a cosine function and its amplitude is dependent on the product of the optical amplitudes from two positions. It has to be pointed out that the proposed scheme provides the phase difference between two positions, whereas the heterodyne detection measures the optical phase φ of the backscattered light. The value $\Delta\varphi$ is intrinsically dependent on the refractive index between $z-\Delta l$ and z, so it is supposed to fluctuate over the distance due to the random profile of the refractive index along the fiber. However, the optical phase φ accumulates as the light propagates along the fiber, so $\varphi(z)$ should change monotonically.

Optics EXPRESS

The DCM algorithm has been applied to retrieve the phase information $\Delta\varphi(z)$ from the signal P_{out} [13]. The reported method is however complicated and vulnerable to system noise [12]. In this paper, the IQ demodulation is used to retrieve the phase difference. This method requires in-phase and quadrature components, and the arctangent of their ratio gives the phase information.

The KK relation describes the relation between the real and imaginary parts of a complex function, so that one part can be determined by the other:

$$\begin{cases} S_R = \frac{1}{\pi} p.v. \int_{-\infty}^{\infty} \frac{S_I(t)}{t-x} dx \\ S_I = -\frac{1}{\pi} p.v. \int_{-\infty}^{\infty} \frac{S_R(t)}{t-x} dx \end{cases}, \tag{5}$$

where S_R and S_I represent the real and imaginary parts, respectively, and $p.v.$ denotes Cauchy principle value. A mathematical description of the KK relation is essentially the Hilbert transform (HT).

The balanced photodetector offers only one signal that acts as the I component as shown by Eq. (4), and it is a cosine function with a fixed amplitude at a given position. The KK detection is used here to obtain the Q part based on the Kramers-Kronig relation. Since the KK relation can be mathematically expressed by the Hilbert transform (HT) [11], the Q signal is obtained at the HT of P_{out}. And the HT of a cosine function turns out to be a sine function [18]. Therefore, the Q component can be expressed as

$$Q(t,z) = \mathrm{H}[P_{out}(t,z)] = -|A(z)A(z-\Delta l)| \sin[\Delta\varphi(t,z) - 2\pi\Delta l/\lambda]. \tag{6}$$

where H represents the Hilbert transform. As a result, the optical phase can be calculated as

$$\Delta\varphi(t,z) = \tan^{-1}[I(t,z)/Q(t,z)] = \tan^{-1}\{P_{out}(t,z)/\mathrm{H}[P_{out}(t,z)]\}. \tag{7}$$

The phase delay $2\pi\Delta l/\lambda$ induced by the arm length difference Δl can be considered as a constant, and it is neglected in the calculation. Note that the arctangent function provides a value between $-\pi/2$ and $\pi/2$, thus phase unwrapping technique is usually necessary to acquire the true phase information. Then, obtained $\Delta\varphi(t, z)$ can be used to calibrate the strain by Eq. (1).

2.2. Phase error analysis

Measurand error is a key parameter to evaluate the sensing performance of the φOTDR system and it is caused by the measurement noise. Several factors affect the performance in practice. For example, the laser phase noise can induce a phase error [19]. And the phase noise is supposed to be converted into intensity after the IMZI, causing an error in the obtained signal. The intensity error results in a variance of the phase difference $\Delta\varphi$ obtained by the IQ demodulation. The relationship between the laser phase noise and the resultant phase error deserves further analysis. Laser frequency drift and low extinction ratio of the optical pulse also degrade the obtained phase information [20,17]. Even in an optimized φOTDR system, the detection noise, e.g. thermal noise and shot noise, is still inevitable. Consequently, the obtain I and Q components in the proposed scheme will suffer from the detection noise and result in an imprecise phase difference $\Delta\varphi$. According to the error propagation theory [21], the variance of the optical phase, i.e. the phase error, extracted by the IQ demodulation can be expressed as [22]

$$\begin{aligned} \sigma^2_{\Delta\varphi}(t,z) &= \left[\frac{I(t,z)}{I^2(t,z)+Q^2(t,z)}\right]^2 \sigma_I^2 + \left[\frac{Q(t,z)}{I^2(t,z)+Q^2(t,z)}\right]^2 \sigma_Q^2 \\ &\quad -2\frac{I(t,z)Q(t,z)\cdot \mathrm{cov}[I(t,z),Q(t,z)]}{[I^2(t,z)+Q^2(t,z)]^2}, \end{aligned} \tag{8}$$

where ${\sigma_I}^2$ and ${\sigma_Q}^2$represent the noise in I and Q components respectively, and $cov()$ denotes the covariance.

Optics EXPRESS

The detection noise is usually assumed to be a zero-mean Gaussian variable, and the HT causes no change of the its variance [22], so the noise variances in the I and Q components can be considered the same: $\sigma_I{}^2=\sigma_Q{}^2=\sigma_n{}^2$. In addition, previous investigation has proven that the covariance of the I and Q components is negligible when the path imbalance Δl is large enough [23]. Hence the resultant phase variance can be rewritten as:

$$\sigma_{\Delta\varphi}^2(t,z) = \frac{\sigma_n^2}{I^2(t,z) + Q^2(t,z)}, \tag{9}$$

where $\sigma_n{}^2$ denotes the detection noise. It is worth noting that Eq. (9) offers a general expression of the phase variance obtained by the IQ demodulation, because the same result has been derived for the coherent-detection-based φOTDR [17,22].

3. Experiment

3.1. Experiment setup

The experimental setup of the φOTDR system based on an IMZI with a 2×2 coupler is plotted in Fig. 2. A narrowband semiconductor laser (2.9 kHz) is employed as the light source. The continuous wave from the laser is converted into optical pulses with a high extinction ratio by a semiconductor optical amplifier (SOA). Then, the generated pulses get amplified by an Erbium-doped fiber amplifier (EDFA) and a bandpass filter is used to suppress the amplified spontaneous emission from the EDFA. The optical power of the pulses needs to be adjusted by a tunable attenuator in order to avoid modulation instability. A circulator is used to launch the pulse into a single mode fiber and guide the backscattered light from the fiber. As a proof-of-concept, the fiber length is 970 m, but the sensing distance can certainly be longer and the limit is supposed the same as other φOTDR systems based on direct detection. The weak optical beam is boosted by another EDFA and passes through a filter before entering the IMZI scheme. One arm of the interferometer is 3.1 m longer than the other, which determines the gauge length. The two outputs of the IMZI are connected to a balanced photodetector. The pulse repetition rate is 1 kHz and the pulse width is 12 ns. And the bandwidth of the detector is 200 MHz, which is large enough for the pulse width [24]. The obtained signal is digitized at a sampling space of 0.2 m and processed by a computer.

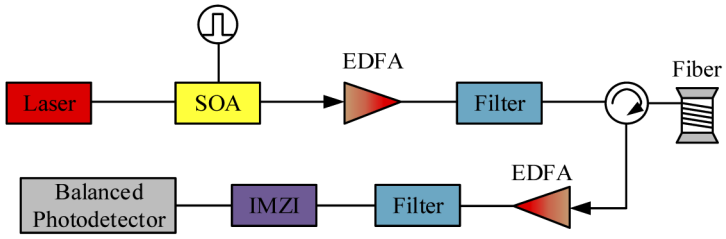

Fig. 2. Experimental setup of a φOTDR system based on an imbalanced Mach-Zehnder interferometer with a 2×2 coupler. For vibration measurement, the fiber section from 924 m to 938 m is perturbed.

3.2. Vibration measurement

In order to realize distributed sensing, a sinusoidal vibration at 200 Hz has been applied to a 14-m long fiber from 924 m through a piezoelectric ceramic transducer (PZT). Like a standard φOTDR system, the upper limit of the frequency response of the proposed scheme is determined by the pulse repetition rate. However, under the same repetition rate, high vibration frequency

Optics EXPRESS

means less sampling points within one period, thus the obtained waveform may be distorted. There are generally five key points in a sinusoidal wave, two of which correspond to maximum and minimum values and the rest possess a value of zero. And the minimum interval between the points should equal one quarter of the vibration period, in other words, the sampling frequency needs to be four times of the vibration frequency. As a result, the 1 kHz pulse repetition rate used in the measurement is supposed to be enough to cover all the five points in the ideal case.

The temporal variations of the obtained signal (I component) at 931.7 m is plotted in Fig. 3(a). The external vibration causes the detected signal oscillates over time, and the Fourier transform of this signal reveals the vibration frequency. However, it is impossible to obtain the vibration amplitude or strain information just based on the obtain signal, the optical phase must be retrieved.

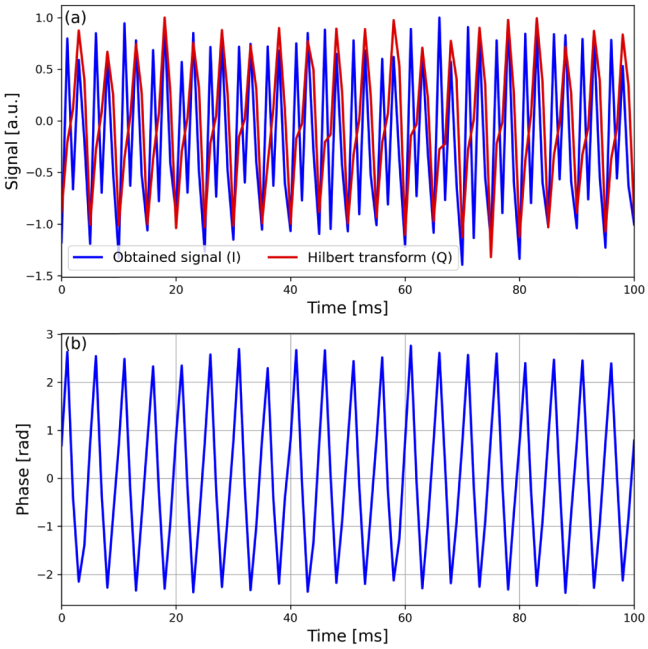

Fig. 3. Vibration caused (a) temporal variations of the obtained signal (I component) and its Hilbert transform (Q component) and (b) Phase difference retrieved by IQ demodulation at 931.7 m.

At first, the Hilbert transform is applied to the acquired signal to obtain the Q component, as shown by the red line in Fig. 3. Then, the phase information $\Delta\varphi(t, z)$ can be retrieved by the IQ demodulation and is presented in Fig. 3(b). Due to the low repetition rate, the obtained curve is closer to a triangular function instead of a perfect sinusoidal function. And the peak-to-peak value changes over time, which can be caused by the detection noise.

The measurement is repeated under different driving voltages of the PZT, so that the tested fiber expenses different strains and the corresponding phase changes can be recorded. The measured phase is plotted as a function of the applied voltage in Fig. 4, and the second x-axis on the top is the corresponding strain calculated according to the datasheet of the PZT. The obtained phase exhibits a linear relationship with the applied strain and the R-squared of the linear fitting is over 0.98. The corresponding slope (31 rad/με) can be obtained from the fitting, and it is normalized to the gauge length (3.1 m) as 10 rad/m/με. This value is similar to the theoretical analysis and some reported experimental results [25,26], validating the functionality of the system.

Optics EXPRESS

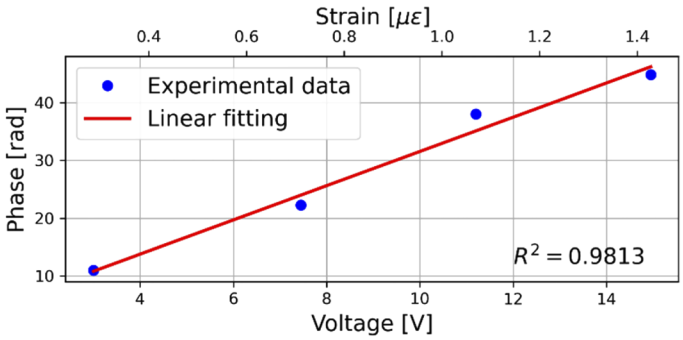

Fig. 4. Measured phase as a function of driving voltage for the PZT and the corresponding strain.

3.3. Phase error

Because of detection noise, the obtained phase of the φOTDR system varies for different measurements under the same environmental conditions, as analyzed in Section II. And the phase variance turns out to be proportional to the summation of I and Q squared at a given position, according to Eq. (9). The in-phase and quadrature components have been expressed respectively in Eqs. (4) and (6). Thus the summation can be calculated as

$$I^2(t,z) + Q^2(t,z) = A^2(z)A^2(z-\Delta l) = I_{opt}(z)I_{opt}(z-\Delta l), \tag{10}$$

where I_{opt}=AA^* denotes the optical intensity of the backscattered light. Since I_{opt} is a random variable, the value of I^2+Q^2 varies along the fiber. Consequently, the obtained phase error is supposed to be a position dependent variable.

To investigate the phase error, the φOTDR measurement is repeated by 1000 times. The phase noise of the employed laser is very small (8 $\mu rad/\sqrt{Hz}$ at 200 Hz for 1 m optical path delay), so its influence on the phase error is negligible. The coherent noise has also limited impact on the sensing performance, because it is highly suppressed due to the high extinction ratio of the optical pulse [27]. Moreover, the whole fiber is well isolated from external stimuli during the measurement. Therefore, it can be safely assumed that the phase variance is mainly caused by detection noise.

Based on the 1000 successive measurements, the I and Q components can be obtained, then the I^2+Q^2 value is calculated along the fiber. The averaged I^2+Q^2 value of a short fiber section is plotted in Fig. 5(a). It demonstrates a stochastic profile and becomes low at some positions, which can be seen as the fading points. The variance of the experimentally obtained phase from the same fiber section is shown in Fig. 5(b). The variance remains below 10^{-1} rad^2 for most part of the fiber, but large variance can be observed at the fading points where the I^2+Q^2 value is low. For example, the variance is about 10^3 rad^2 at 613.5 m because the I^2+Q^2 value is just $\sim 10^4$. On the contrary, a small variance well below 10^{-2} rad^2 is observed at 620 m due to the high I^2+Q^2 value.

The phase error can also be calculated based on Eq. (8) and the detection noise ${\sigma_n}^2$ can be determined from the experimental data. The theoretical analysis matches well with the experimental result, as presented in Fig. 5(b). There exist however large deviations between the two curves at the fading points. The obtained phases at these positions are supposed to be inaccurate, because the local SNR is low due to the small I^2+Q^2 value. Therefore, the phase unwrapping of the unreliable results introduces more errors. Consequently, the phase variance obtained by experiment is several orders of magnitude larger, whereas the error due to the phase unwrapping is not considered by the theoretical analysis, so the predicted error is still

Optics EXPRESS

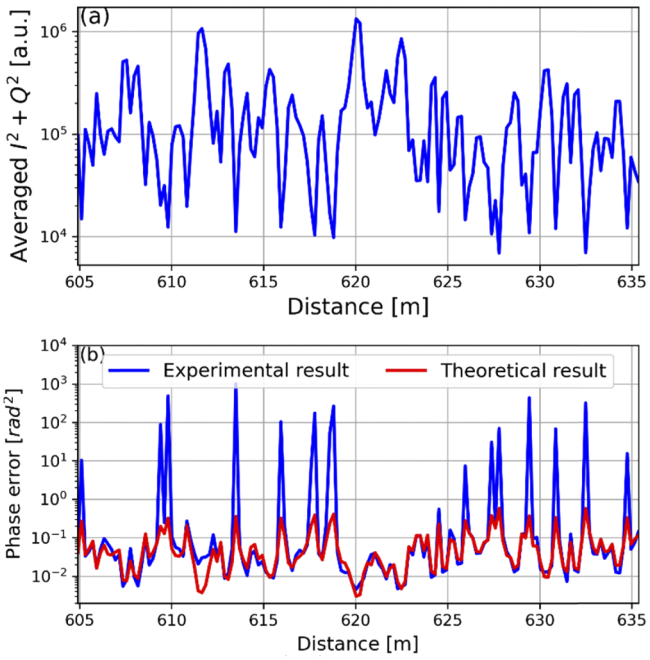

Fig. 5. Longitudinal profile of (a) the averaged I^2+Q^2 value and (b) phase error obtained by experiment and theoretical analysis along a shot section of the fiber from 605 m to 636 m.

comparatively low. A similar result has been observed for a coherent-detection-based φOTDR system [22].

The probability density function (PDF) is used to statistically describe the overall phase noise along the fiber owing to its random nature. The PDFs of the phase error are shown in Fig. 6 and (a) good agreement between the experiment and the theoretical work can be observed. As shown in Fig. 5(b), the theoretical prediction matches very well with the experimental result for most part of the fiber (non-fading sections). And the phase error in these parts gives rise to the PDF peak shown in Fig. 6. At the fading points, however, the experimental result exhibits a non-zero over 1 rad^2 due to the phase unwrapping errors.

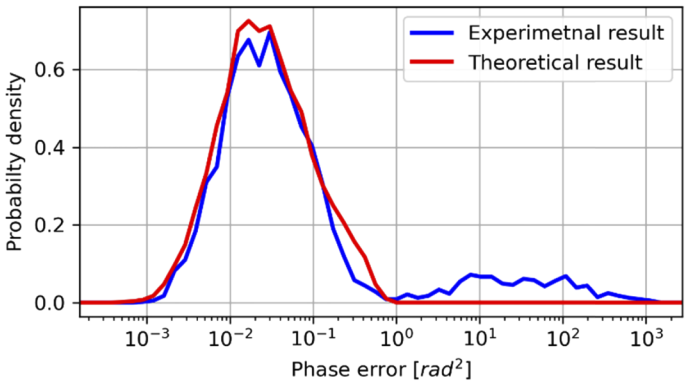

Fig. 6. Probability density function of the phase error obtained experimentally and theoretically for a φOTDR system based on an imbalanced Mach-Zehnder interferometer with a 2×2 coupler.

Optics EXPRESS

4. Discussion

The classical IMZI-based φOTDR system employs a 3×3 coupler as the interferometer output and 3 photodetectors to acquire light [5]. The detected signal can be expressed as [22]

$$\begin{cases} P_1(t,z) = P_{DC}(z) - P_{AC}(z)\sin[\Delta\varphi(t,z) + 2\pi/3] \\ P_2(t,z) = P_{DC}(z) - P_{AC}(z)\sin[\Delta\varphi(t,z)] \\ P_3(t,z) = P_{DC}(z) - P_{AC}(z)\sin[\Delta\varphi(t,z) - 2\pi/3] \end{cases}, \tag{11}$$

where P_{DC}=[$I_{opt}(z)$+$I_{opt}(z-\Delta l)$]/6 and P_{AC}=$A(z)\cdot A(z-\Delta l)$/3. The phase information can be extracted from the detected signal by the DCM algorithm or IQ demodulation. In practice, it is impossible for the used detectors to possess exactly the same responsibility and noise character. The slight difference of the photodetectors can induce a measurement error. The performance of such a scheme is also limited by the asymmetry of the coupler [28]. The scheme based on 2×2 coupler is supposed to be more robust against these factors and its scheme is comparatively simple and low-cost. In addition, it acquires and processes less data, so that it is more attractive for practical applications.

Previous studies on fiber point sensors have revealed that the fiber interferometers using 3×3 coupler demonstrate better performance than using 2×2 coupler, because the former scheme avoids the signal fading problem [29,30]. However, there exists no such investigations for the φOTDR sensing as far as we know. Here, the IMZI-based φOTDR systems using 2×2 and 3×3 couplers are compared in terms of the phase error. To guarantee a fair comparison, IQ demodulation is used to retrieve the phase for the scheme based on 3×3 coupler. The corresponding I and Q components are obtained from the detected signal and are written as

$$\begin{cases} I_{IMZI}(t,z) = -\frac{1}{2}P_1(t,z) + P_2(t,z) - \frac{1}{2}P_3(t,z) \\ Q_{IMZI}(t,z) = -\frac{\sqrt{3}}{2}P_1(t,z) + \frac{\sqrt{3}}{2}P_3(t,z) \end{cases}. \tag{12}$$

And the corresponding phase variance is expressed as [21]

$$\sigma'^2_{\Delta\varphi}(t,z) = \frac{1.5\sigma_n^2}{I^2(t,z) + Q^2(t,z)}. \tag{13}$$

The coefficient 1.5 is caused by the accumulation of detection noise from the 3 photodetectors. Just like the 2×2 coupler-based system, Eq. (13) shows that the phase error is proportional to the value of I^2+Q^2. According to Eqs. (10) and (11), the I^2+Q^2 can be expressed as the product of the optical intensity at two positions as $I_{opt}(z)\cdot I_{opt}(z-\Delta l)$/4. However, the I^2+Q^2 value for the 2×2 coupler-based system is $I_{opt}(z)\cdot I_{opt}(z-\Delta l)$ as presented by Eq. (9). As a result, the simple scheme is expected to offer a smaller phase error, only 1/6 of the 3×3 coupler-based system, under the same condition. This difference is due to the coupling ratio of the different couplers and the different methods to obtain the I and Q components. It is important to note that the 3×3 coupler indeed avoids the fading problem because the experimentally obtained phase variance demonstrates no unwrapping error [21].

It can be concluded that the 2×2 coupler-based system in general provides a smaller measurement error by comparing Eqs. (8) and (12), but it suffers from signal fading which causes large errors. Consequently, advanced fading removal techniques, such as rotated-vector-sum, spectrum extraction and remix method and M-degree summation of incoherent scattered light [31–33], need to be adapted to the proposed system in order to suppress the fading effect. Novel phase unwrapping methods may also help alleviate the related error.

Optics EXPRESS

5. Conclusion

In this paper, the application of a Kramers-Kronig receiver to a φOTDR system based on direct detection has been proposed, theoretically analyzed and experimentally demonstrated. The in-phase and quadrature components are obtained by the KK receiver and IQ demodulation is employed to retrieve the phase information. The sensing system relies on an IMZI for phase extraction, uses a 2×2 coupler as the output of the interferometer and the signal is detection by a balanced photodetector. This scheme is much simpler than the classical setup which requires a 3×3 coupler and 3 identical photodetectors, and it provides an economic solution to practical applications. However, the IMZI with a 2×2 coupler suffers from signal fading just like most of the φOTDR systems, and this problem needs to be solved in future work.

Funding

Zentrale Innovationsprogramm Mittelstand (ZF4044230RH9).

Acknowledgments

The research project was carried out in the framework of the Zentrale Innovationsprogramm Mittelstand (ZF4044230RH9, project acronym "FoLO"). It was supported by the Federal Ministry for Economic Affairs and Energy (BMWi) on the basis of a decision by the German Bundestag. The authors thank Marcus Schukar and Sven Münzenberger at BAM for their technical support and thank all the partners in the FoLO project for helpful discussion.

Disclosures

The authors declare no conflicts of interest.

References

1. A. H. Hartog, *An Introduction to Distributed Optical Fibre Sensors* (CRC, 2017).
2. P. Ma, K. Liu, Z. Sun, J. Jiang, S. Wang, T. Xu, Z. Xu, and T. Liu, "Distributed single fiber optic vibration sensing with high frequency response and multi-points accurate location," Opt. Lasers Eng. **129**, 106060 (2020).
3. Z. Wang, L. Zhang, S. Wang, N. Xue, F. Peng, M. Fan, W. Sun, X. Qian, J. Rao, and Y. Rao, "Coherent Φ-OTDR based on I/Q demodulation and homodyne detection," Opt. Express **24**(2), 853–858 (2016).
4. Z. Zhong, F. Wang, M. Zong, Y. Zhang, and X. Zhang, "Dynamic measurement based on the linear characteristic of phase change in Φ-OTDR," IEEE Photonics Technol. Lett. **31**(14), 1191–1194 (2019).
5. A. Masoudi, M. Belal, and T. P. Newson, "A distributed optical fibre dynamic strain sensor based on phase-OTDR," Meas. Sci. Technol. **24**(8), 085204 (2013).
6. C. Wang, C. Wang, Y. Shang, X. Liu, and G. Peng, "Distributed acoustic mapping based on interferometry of phase optical time-domain reflectometry," Opt. Commun. **346**, 172–177 (2015).
7. Z. Pan, K. Liang, Q. Ye, H. Cai, R. Qu, and Z. Fang, "Phase-sensitive OTDR system based on digital coherent detection," Proc. SPIE **8311**, 83110S (2011).
8. M. Zabihi, X. Chen, T. Zhou, J. Liu, F. Wang, Y. Zhang, and X. Zhang, "Compensation of optical path difference in heterodyne Φ-OTDR systems and SNR enhancement by generating multiple beat signals," Opt. Express **27**(20), 27488–27499 (2019).
9. A. Mecozzi, C. Antonelli, and M. Shtaif, "Kramers–Kronig coherent receiver," Optica **3**(11), 1220–1227 (2016).
10. A. Mecozzi, C. Antonelli, and M. Shtaif, "Kramers–Kronig receivers," Adv. Opt. Photonics **11**(3), 480–517 (2019).
11. J. Jiang, Z. Wang, Z. Wang, Y. Wu, S. Lin, J. Xiong, Y. Chen, and Y. Rao, "Coherent Kramers-Kronig receiver for Φ-OTDR," J. Lightwave Technol. **37**(18), 4799–4807 (2019).
12. A. Masoudi and T. P. Newson, "High spatial resolution distributed optical fiber dynamic strain sensor with enhanced frequency and strain resolution," Opt. Lett. **42**(2), 290–293 (2017).
13. H. Qian, B. Luo, H. He, X. Zhang, X. Zou, W. Pan, and L. Yan, "Phase demodulation based on DCM algorithm in Φ-OTDR with self-interference balance detection," IEEE Photonics Technol. Lett. **32**(8), 473–476 (2020).
14. X. Lu and P. J. Thomas, "Numerical modeling of Fcy OTDR sensing using a refractive index perturbation approach," J. Lightwave Technol. **38**(4), 974–980 (2020).
15. Z. Sha, H. Feng, and Z. Zeng, "Phase demodulation method in phase-sensitive OTDR without coherent detection," Opt. Express **25**(5), 4831–4844 (2017).
16. C. D. Butter and G. B. Hocker, "Fiber optics strain gauge," Appl. Opt. **17**(18), 2867–2869 (1978).
17. H. Gabai and A. Eyal, "On the sensitivity of distributed acoustic sensing," Opt. Lett. **41**(24), 5648–5651 (2016).

Optics EXPRESS

18. T. H. Crystal, "The Hilbert transform as an iterated Fourier transform: comment the Hilbert transform as an iterated Laplace transform," IEEE Trans. Aerosp. Electron. Syst. **AES-4**(2), 315 (1968).
19. G. Yang, X. Fan, S. Wang, B. Wang, Q. Liu, and Z. He, "Long-range distributed vibration sensing based on phase extraction from phase-sensitive OTDR," IEEE Photonics J. **8**(3), 1–12 (2016).
20. Q. Yuan, F. Wang, T. Liu, Y. Liu, Y. Zhang, Z. Zhong, and X. Zhang, "Compensating for influence of laser-frequency-drift in phase-sensitive OTDR with twice differential method," Opt. Express **27**(3), 3664–3671 (2019).
21. J. Oksanen and T. Sarjakoski, "Error propagation of DEM-based surface derivatives," Comput. Geosci. **31**(8), 1015–1027 (2005).
22. X. Lu, M. A. Soto, P. J. Thomas, and E. Kolltveit, "Evaluating phase errors in phase-sensitive optical time-domain reflectometry based on I/Q demodulation," J. Lightwave Technol. **38**(15), 4133–4141 (2020).
23. H. Storch and F. W. Zwiers, "Complex eigentechniques," in *Statistical Analysis in Climate Research*, H. Storch and F. W. Zwiers, eds. (Cambridge University, 2003).
24. X. Lu, M. A. Soto, L. Zhang, and L. Thévenaz, "Spectral properties of the signal in phase-sensitive optical time-domain reflectometry with direct detection," J. Lightwave Technol. **38**(6), 1513–1521 (2020).
25. G. Tu, X. Zhang, Y. Zhang, F. Zhu, L. Xia, and B. Nakarmi, "The development of an φ-OTDR system for quantitative vibration measurement," IEEE Photonics Technol. Lett. **27**(12), 1349–1352 (2015).
26. Y. Dong, X. Chen, E. Liu, C. Fu, H. Zhang, and Z. Lu, "Quantitative measurement of dynamic nanostrain based on a phase-sensitive optical time domain reflectometer," Appl. Opt. **55**(28), 7810–7815 (2016).
27. H. F. Martins, S. Martin-Lopez, P. Corredera, M. L. Filograno, O. Frazão, and M. González-Herráez, "Coherent noise reduction in high visibility phase-sensitive optical time domain reflectometer for distributed sensing of ultrasonic waves," J. Lightwave Technol. **31**(23), 3631–3637 (2013).
28. Z. Zhao, M. S. Demokan, and M. MacAlpine, "Improved demodulation scheme for fiber optic interferometers using an asymmetric 3×3 coupler," J. Lightwave Technol. **15**(11), 2059–2068 (1997).
29. S. K. Sheem, "Optical fiber interferometers with [3×3] directional couplers: analysis," J. Appl. Phys. **52**(6), 3865–3872 (1981).
30. S. K. Sheem, T. G. Giallorenzi, and K. Koo, "Optical techniques to solve the signal fading problem in fiber interferometers," Appl. Opt. **21**(4), 689–693 (1982).
31. D. Chen, Q. Liu, and Z. He, "Phase-detection distributed fiber-optic vibration sensor without fading-noise based on time-gated digital OFDR," Opt. Express **25**(7), 8315–8325 (2017).
32. Y. Wu, Z. Wang, J. Xiong, J. Jiang, S. Lin, and Y. Chen, "Interference fading elimination with single rectangular pulse in Φ-OTDR," J. Lightwave Technol. **37**(13), 3381–3387 (2019).
33. S. Lin, Z. Wang, J. Xiong, Y. Fu, J. Jiang, Y. Wu, Y. Chen, C. Lu, and Y. Rao, "Rayleigh fading suppression in one-dimensional optical scatters," IEEE Access **7**, 17125–17132 (2019).